

UC Davis

UC Davis Previously Published Works

Title

Wind energy variability and links to regional and synoptic scale weather

Permalink

<https://escholarship.org/uc/item/1vc7j0fr>

Journal

Climate Dynamics, 52(7-8)

ISSN

0930-7575

Authors

Millstein, Dev
Solomon-Culp, Joshua
Wang, Meina
[et al.](#)

Publication Date

2019-04-01

DOI

10.1007/s00382-018-4421-y

Peer reviewed



Electricity Markets & Policy
Energy Analysis & Environmental Impacts Division
Lawrence Berkeley National Laboratory

Wind Energy Variability and Links to Regional and Synoptic Scale Weather

J Dev Millstein^a, Joshua Solomon-Culp^a, Meina Wang^{a,b}, Paul Ullrich^{a,b},
Craig Collier^c

^a Lawrence Berkeley National Laboratory, Berkeley, CA, USA

^b University of California, Davis, Davis, CA, USA

^c DNV GL, San Diego, CA, USA

August 2018

This is a pre-print version of an article published in *Climate Dynamics*.
DOI: <https://doi.org/10.1007/s00382-018-4421-y>



This work was funded by the California Energy Commission under the Electric Program Investment Charge Grant, EPC-15-068: Understanding and Mitigating Barriers to Wind Energy Expansion in California.

DISCLAIMER

This document was prepared as an account of work sponsored by the United States Government. While this document is believed to contain correct information, neither the United States Government nor any agency thereof, nor The Regents of the University of California, nor any of their employees, makes any warranty, express or implied, or assumes any legal responsibility for the accuracy, completeness, or usefulness of any information, apparatus, product, or process disclosed, or represents that its use would not infringe privately owned rights. Reference herein to any specific commercial product, process, or service by its trade name, trademark, manufacturer, or otherwise, does not necessarily constitute or imply its endorsement, recommendation, or favoring by the United States Government or any agency thereof, or The Regents of the University of California. The views and opinions of authors expressed herein do not necessarily state or reflect those of the United States Government or any agency thereof, or The Regents of the University of California.

Ernest Orlando Lawrence Berkeley National Laboratory is an equal opportunity employer.

COPYRIGHT NOTICE

This manuscript has been authored by an author at Lawrence Berkeley National Laboratory under Contract No. DE-AC02-05CH11231 with the U.S. Department of Energy. The U.S. Government retains, and the publisher, by accepting the article for publication, acknowledges, that the U.S. Government retains a non-exclusive, paid-up, irrevocable, worldwide license to publish or reproduce the published form of this manuscript, or allow others to do so, for U.S. Government purposes.

Wind Energy Variability and Links to Regional and Synoptic Scale Weather

Dev Millstein^{*a}, Joshua Solomon-Culp^a, Meina Wang^{a,b}, Paul Ullrich^{a,b}, Craig Collier^c

a Lawrence Berkeley National Laboratory, Berkeley, CA, USA

b University of California, Davis, Davis, CA, USA

c DNV GL, San Diego, CA, USA

* corresponding author: dmillstein@lbl.gov, (510) 486-4556

PRE-PRINT of article in *Climate Dynamics*:

Millstein, D., Solomon-Culp, J., Wang, M., Ullrich, P. and Collier, C., 2019. Wind energy variability and links to regional and synoptic scale weather. *Climate Dynamics*, 52(7), pp.4891-4906. <https://doi.org/10.1007/s00382-018-4421-y>

Abstract

The accurate characterization of seasonal and inter-annual site-level wind energy variability is essential during wind project development. Understanding the features and probability of low-wind years is of particular interest to developers and financiers. However, a dearth of long-term, hub-height wind observations makes these characterizations challenging, and thus techniques to improve these characterizations are of great value. To improve resource characterization, we explicitly link wind resource variability (at hub-height, and at specific sites) to regional and synoptic scale wind regimes. Our approach involves statistical clustering of high-resolution modeled wind data, and is applied to California for a period covering 1980 – 2015. With this approach, we investigate the unique meteorological patterns driving low and high wind years at five separate wind project sites. We also find wind regime changes over the 36-year period consistent with global warming: wind regimes associated with anomalously hot summer days increased at half a day per year and stagnant conditions increased at one third days per year. Despite these changes, the average annual resource potential remained constant at all project sites. Additionally, we identify correlations between climate modes and wind regime frequency, a linkage valuable for resource characterization and forecasting. Our general approach can be applied in any location and may benefit many aspects of wind energy resource evaluation and forecasting.

Keywords

Wind energy; Wind resource inter-annual variability; Regional climate

1 Introduction

Technology improvements and cost reductions have helped reduce wind energy prices to record lows and are the primary drivers of the expansion of wind energy deployment globally (GWEC 2017). Through this expansion, wind energy has begun to provide air quality, public health, and greenhouse gas emission benefits by substituting for the use of fossil fuels in the electric sector (Cullen 2013; Kaffine et al. 2013; Millstein et al. 2017; Siler-Evans et al. 2013). Looking forward, wind energy growth may be further encouraged as wind energy can feasibly play an important role in long term global efforts to reduce electric sector greenhouse gas emissions (Barthelmie and Pryor 2014; Cochran et al. 2014; GWEC 2017; Luderer et al. 2014). With this expansion in wind energy, the assessment of wind resource variability may become more critical for three reasons. One, long term planners will have greater need to understand the variability of wind resources expected to come online. Two, the development of many new project sites combined with the potential use of higher towers could lead to project-level resource variability that has different characteristics than expected based on previous experience. Three, understanding and forecasting short-term variability at the project level can help reduce challenges that arise with high levels of wind penetration, such as the need for increased reserve margins and inefficient operation of non-wind generators (Albadi and El-Saadany 2010; Archer et al. 2017; Xie et al. 2011).

The assessment of wind energy resources crosses multiple time and geographic scales. At the broadest scope, variability of wind resources is tracked across countries and continents informing project developers and the broader energy community about the performance of wind farms and the availability of wind power. For example, Archer and Jacobson (2013) characterize global wind energy resources showing these resources are sufficient to meet energy demands in most regions at annual scales. Many studies have characterized wind resources, and trends in wind resources, at a regional level, e.g., Pryor et al. (2006) for Europe, Pryor et al. (2009) and Yu et al. (2015) for the U.S., Yu et al. (2016) for China, and McVicar et al. (2008) for Australia. At mid-latitudes, Pryor et al. (2009) and McVicar et al. (2008) compared long term historical trends in wind speeds between reanalysis data and surface observations, both finding that negative trends over the past few decades in surface wind speed observations were not replicated in reanalysis data. Vautard et al. (2010) showed changes to surface roughness is possible explanation for the trends in observed surface wind speeds. Pryor et al. (2006) found a mixed result for historical trends in California wind speeds with some locations showing decreasing wind speeds and others showing increasing wind speeds.

Many analyses have sought to link wind resource variation with climate change. Wind resource variability has also been linked to climate modes (Berg et al. 2013; Clifton and Lundquist 2012; Li et al. 2010; Yu et al. 2016). Globally, Karnauskas et al. (2017) analyze simulated changes to wind resources across ten climate models, finding robust reductions to wind power in northern mid-latitudes. Regional studies show a variety of results. Sherman et al. (2017) find that two key regions in China have already seen reductions of ~15% in wind resources over the past decades and that this reduction was associated with climate change but modulated by climate modes. Examining wind speeds climatology in the U.S. between 1979 and 2011, Yu et al. (2015) find

positive long term trends across much of the western half of the U.S., but negative trends in the east and in some parts of California. Yu et al. (2015) also find that climate modes influence seasonal wind speeds across the U.S. Looking forward, Pryor and Barthelmie (2011) find that, in the U.S., simulated future wind resources remain similar to the present day, however, Haupt et al. (2016) find that future wind speeds vary by up to 10% depending on the season and U.S. region. Climate change may impact other aspects of wind energy generation, such as changes to icing frequency and extreme events (Pryor and Barthelmie 2013) or changes to diurnal or seasonal cycles of wind resources (Goddard et al. 2015). In California, Duffy et al. (2014) and Wang et al. (2018) ran independent, high resolution simulations and found that future wind resources are diminished during the fall and winter. Wang et al. (2018) found that future Californian wind resources increase during the summer. Overall, assessing the likely impact of climate change on wind energy is an active area of study.

At the site level, resource assessment is necessary during early project development, and is commonly performed using “measure-correlate-predict” methods, an approach used to overcome the dearth of local long-term hub-height wind measurements (Carta et al. 2013). Accurate, site-level, quantification of resource variability, especially characterization of low wind years, is essential information for project developers and financiers (Bailey and Kunkel 2015; Bolinger 2017; Tindal 2011). Once a project is in operation, measures of variability in wind energy resource are needed to determine its performance. Staffell and Green (2014) and Olauson et al. (2017), for example, used metrics of wind resource variability to determine how age impacts performance across fleets of wind turbines.

As the above examples demonstrate, improving the understanding of wind resource variability can help support many aspects of wind power development and operations. In addition to the needed assessment of site-level variability, regional assessments of the links between wind resources and climate change and climate modes can help inform discussions related to wind energy policies and regional land-use decisions.

One approach to analyzing variability in wind speed and direction is to use statistical clustering techniques to group together days or hours with similar meteorological properties. This approach can help link variation in wind seen at individual sites to meteorological patterns at larger geographic and multiple temporal scales, providing insight into the mechanisms for, and potentially predictability of, such variation. For example, Berg et al. (2013) find a shift in southern California winter surface wind regimes during El Niño, and other works have aimed to improve regional descriptions of surface wind climatology (Chadee and Clarke 2015; Conil and Hall 2006; Jiménez et al. 2009; Ludwig et al. 2004; Seefeldt et al. 2007; Zaremba and Carroll 1999). Clustering techniques are used to identify wind patterns associated with certain air pollution profiles (Beaver and Palazoglu 2009; Darby 2005; Jin et al. 2011). Although to date, clustering approaches have mainly been applied to surface level wind fields, Clifton and Lundquist (2012) cluster speed and direction measurements observed at a tall tower in Colorado, finding links in wind resource characteristics to El Niño, and suggest the clustering technique might aid in site-level wind resource estimation. Also, Gibson and Cullen (2015) link wind measurements at a tower in southern New Zealand to typical synoptic scale patterns.

This study extends and adapts clustering techniques to the analysis of hub-height wind resources so as to (1) directly link site-level wind profiles to synoptic scale meteorological conditions, (2) illuminate the unique reasons for variation in annual generation potential at specific wind project sites, and (3) provide insight into the impacts of climate mode intensity and the impacts of climate change on wind resources. The study relies on 36 years, between 1980 – 2015, of wind fields modeled 100 meters above ground level developed by DNV GL (a large energy consultancy) and optimized for wind energy analysis. The model is finely resolved (4 by 4 km), covers the full state of California, and was carefully validated with available observational data. Results focus on five of the largest wind farms in the state, and provide site-level insight into wind resource variability. While this demonstration focuses on California, the generalized approach can be applied in any location, and shows potential to help improve wind resource assessment and provide benefit to wind energy operations and to other fields, such as atmospheric science and air quality engineering.

2 Methodology

2.1 Description of DNV GL virtual meteorology product

DNV GL (Det Norske Veritas Germanischer Lloyd) is a large energy consultancy firm that supports wind power development efforts throughout the world. For the purpose of this research, DNV GL provided its Virtual Met product covering 1980 – 2015 and focused on California. The Virtual Met product is a dynamically-downscaled regional model product based on MERRA-2 input data and is designed specifically to provide wind farm developers with accurate characterizations of wind power resources at existing and prospective project sites. The downscaling is accomplished in two steps: First, the Weather Research and Forecasting (WRF) model is used to dynamically downscale MERRA2 to 20 km resolution across a domain covering California, and second, an analog-based ensemble downscaling method is used to refine the resolution to 4 km. The coarse 20 km WRF simulation was run for the full domain and time period, and this coarse simulation was then downscaled across all hours of the simulation. The downscaling is based on training data created from a single year's WRF simulation at 4 km on a rotated grid to minimize offshore portions of the domain. DNV GL uses a proprietary combination of parameterizations of WRF for seeding its Analog Ensemble system. Times outside the training period are matched to a set of times within the training period by matching meteorological characteristics across the coarse data sets. These matching times are called 'analogs' and the downscaled solution is based on a combination of the high-resolution data corresponding to the coarse analogs. This method is based on prior studies (Delle Monache et al. 2013; Delle Monache et al. 2011) and is described further in Wang et al. (2018). The 4-km resolution used here is sufficient for our purposes of linking site-level temporal resource variability to larger-scale meteorological processes, although higher resolution would be desired when developing operational resource assessments. The Virtual Met product provides wind speeds and directions at multiple heights above ground level, including 10 m and 100 m. We used 100 m height above ground to represent hub-height in this work and 10 m height to represent surface winds. The 100 m hub-height chosen is based on expectations that average

hub-height for onshore projects in the U.S. will increase over time, up from ~80 m in 2014 to ~115 m in 2030 (Wiser et al. 2016).

Wang et al. (2018) evaluate the Virtual Met product in comparison to surface wind speed observations as well as in comparison to reanalysis products MERRA2, CFSR, and NARR. This evaluation shows that the Virtual Met product has the lowest bias of any of the products tested during spring and summer (the period of high wind resources), and similar biases to the other products during fall and winter. Specifically, Wang et al. (2018) report biases for the Virtual Met product of 0.02 m s^{-1} for March through May, -0.03 m s^{-1} for June through August, 0.40 m s^{-1} for September through November, and 0.56 m s^{-1} for December through February. As mentioned in the introduction of the paper, there is a dearth of long term hub-height wind measurements available for comparison, and thus a detailed evaluation of the quality of the Virtual Met products hub-height wind speeds is not available. Wang et al. (2018) do present a detailed comparison of hub-height wind speeds between reanalysis products and the Virtual Met product. Compared to the other products, the Virtual Met product has a shift towards higher wind speeds at each of the five wind project sites highlighted. This increase in higher speed wind frequencies is likely due to the relatively fine resolution of the Virtual Met product and the fact that wind projects are generally sited at locations with local maximum wind speeds.

2.2 Description of clustering approach

We first split California into two separate domains, one centered on central California, including the Shiloh and Altamont Pass wind farms, and one centered on southern California, including the Alta, San Geronio, and Ocotillo wind farms (Fig. 1). We developed a separate, independent, set of clusters for each of the domains. Clusters developed in the central domain are labeled “C” followed by an identifying number 1 – 10. Clusters developed in the southern domain are labeled “S,” and also followed by an independent identifying number 1 – 10. The identifying numbers are not used in this work for anything other than identification and are effectively arbitrary in their order. We classified each 24-hour period (from January 1st, 1980 through December 31st, 2015) as a cluster type. Thus, every day in the time period was classified as one of 10 clusters in the central California domain and one of 10 clusters in the southern California domain.

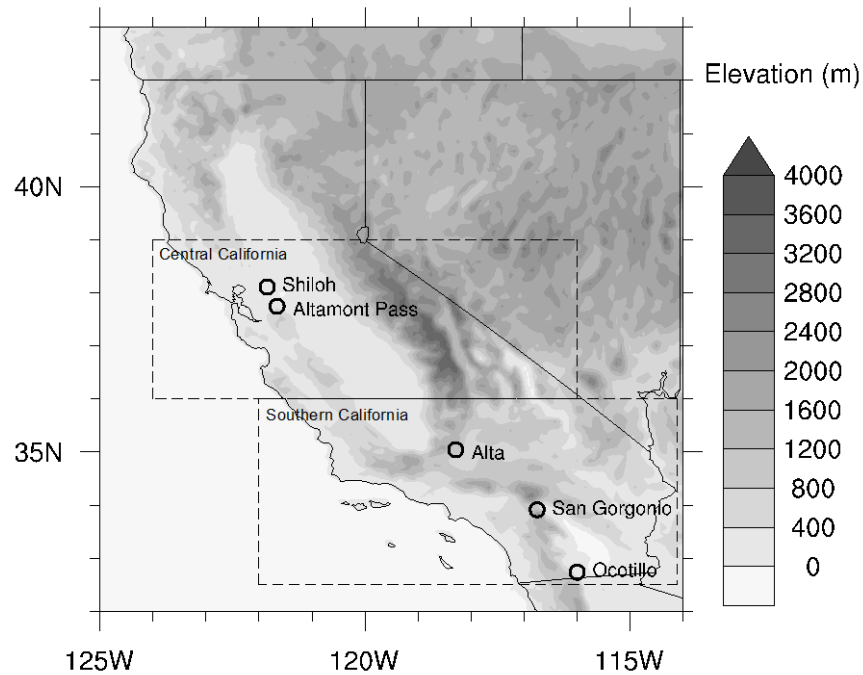


Fig. 1 The central and southern California domains and the location of five major wind development sites. The clustering was accomplished through a two-step process (Fig. 2). First, we reduced the dimensionality of the problem using principal components analysis (PCA), and second, we applied an agglomerative clustering algorithm to the principal component multipliers (the “scores” or “weights” of the PCA process). The approach taken here broadly builds on and extends previous clustering efforts (Beaver and Palazoglu 2009; Berg et al. 2013; Conil and Hall 2006; Darby 2005; Jin et al. 2011; Ludwig et al. 2004).

PCA allows spatial data, at any particular time, to be represented by a mean spatial pattern plus the sum of a limited number of weighted principal spatial patterns. Ludwig et al. (2004) and Jin et al. (2011) provide useful explanations related to PCA’s application to wind fields. From the PCA, we kept the first 10 weights of the principal spatial patterns as these first 10 principal components accounted for greater than 80% of the total variance in wind profiles within each domain, and additional weights would have added less than 1% to the explanation of the variance. Thus, the dimensionality of each hour was reduced from 2-component (east-west vector u and north-south vector v) modeled wind outputs at hub height across all grid cells (~ 8500 in each domain) to 10 PCA weights. The PCA weights were then grouped together by 24-hour periods to form the input for the agglomerative clustering process. Thus, each day, for each domain, is categorized as a particular cluster based on a set of (24×10) 240 PCA scores that describe the profile of wind speed and direction over the course of the day and across the domain.

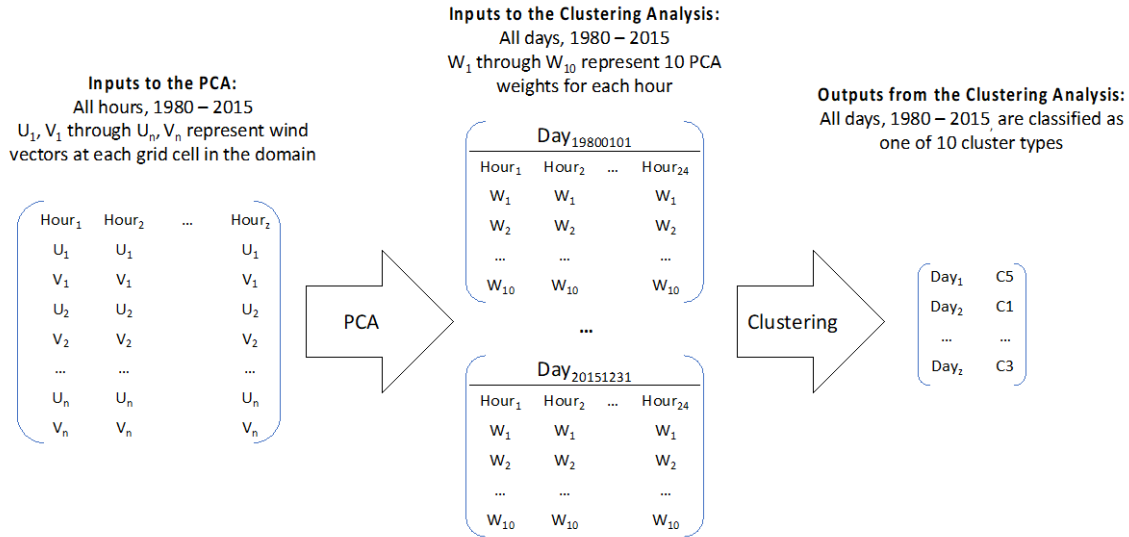


Fig. 2 The PCA and Clustering process ingests wind speeds at each grid cell in the domain and classifies each day as one of ten types

We performed the cluster analysis using a hierarchical clustering technique, specifically agglomerative clustering using Ward’s method (Ward Jr 1963). Agglomerative clustering begins with each ‘observation,’ in this case, each day, classified as its own cluster. Observations are then merged together into larger groups based on minimizing a criterion (Ward’s method minimizes the variance of the clusters being merged) until the predetermined number of total clusters is reached. The ‘right’ total number of clusters varies by application, and in this case, was determined by visually inspecting the regional wind profiles (similar to Fig. 3) after repeatedly running the clustering algorithm while varying the targeted number of clusters. We found, for example, that the use of 5 clusters did not portray the full range of patterns found with 10 clusters, and the set of 15 clusters contained clusters with similar wind profiles to each other. In other words, using 15 clusters identified differences between clusters that were subtler than needed for our application. While our approach was sufficient for our analysis, it may be desirable to iteratively optimize the number of total clusters for specific applications such as short-term forecasting.

The PCA and cluster analyses required the use of specialized computing resources. The PCA included developing and processing an extremely large matrix including columns representing 315,552 hours and rows representing ~8,500 grid cells (the total cells differed slightly between the central and southern domain). Therefore, we used the large memory nodes on the Haswell computer within the U.S. Department of Energy National Energy Research Scientific Computing Center (NERSC). The PCA and agglomerative clustering methods were implemented using the publically available Scikit-learn algorithms (Pedregosa et al. 2011).

2.3 Description of synoptic scale analysis

The synoptic-scale is defined as a horizontal scale on the order of 1000 km or more. We analyzed the seasonal mean anomaly fields that are associated with a sample of clusters (as

shown at the end of section 3). The analyzed fields include 700-hPa geopotential height, which is defined as the height of 700-hPa isobar surfaces above mean sea level, as well as the surface pressure, and 2-meter air temperature. The synoptic scale data is from the MERRA2 reanalysis product, (Gelaro et al. 2017; GES 2017). We chose to look at the 700-hPa geopotential height field since it is reflective of the general circulation pattern: wind flow at this pressure level is largely geostrophic and hence follows constant geopotential contours. The surface pressure field also impacts local wind speeds due to pressure gradient, which is closely associated with surface air temperature changes. Three steps were used to find the seasonal anomaly for each cluster. First, the monthly mean geopotential height, surface pressure, and 2-meter air temperature were calculated across the full-time period. Second, the anomaly fields on days categorized as the particular cluster of interest were calculated by subtracting the long-term monthly mean fields from the daily mean values. Finally, the seasonal averaged anomaly fields were calculated across all the anomaly values within the cluster and season of interest and across the full-time period.

2.4 Power curve and capacity factor

To analyze wind energy generation potential at each site, wind speeds output from the Virtual Met product were converted to wind energy generation potential using idealized power curves. This generation potential represents a lossless potential, and does not account for wake or electrical losses. Wind speeds were transformed at each location and at each hour using the normalized power curves presented in the Wind Integration National Dataset (WIND) Toolkit (Draxl et al. 2015). Different power curves were applied at each site based on the classifications within the WIND Toolkit, specifically the International Electrotechnical Commission (IEC) class 3, 2, 3, 2, and 1 turbine curves were applied to Shiloh, Altamont Pass, Alta, San Geronio, and Ocotillo, respectively.

2.5 Long-term temporal trends in cluster frequency

For each cluster a linear regression was developed with the independent variable being year and the dependent variable being annual occurrence of the cluster (section 6). The p-value for the slope determines whether the slope is significantly different from zero at the 95% confidence level. However, autocorrelation of the errors in an ordinary least squares estimation can lead to an underestimate of the standard errors. We examined the partial autocorrelation function (shown in Supplemental Fig. 3) for the clusters with significant trends over time (C7 and C9) and found C7 exhibited significant auto-correlation at lag 1. To account for the autocorrelation we used the Cochrane-Orcutt procedure (Cochrane and Orcutt 1949) to calculate a new p-value for the slope of C7. The Cochrane-Orcutt procedure removes the influence of lag 1 correlation and produces correct standard errors. The original p-value of the C7 slope was 0.003 and the p-value for the slope after applying the Cochrane-Orcutt procedure was 0.012. Thus, after correcting for autocorrelation, the slope of C7 was still found to be significant. The slope of C9 was also found to be significant at the 95% confidence level, having a p-value of 0.039. Given that no lag was found to have significant autocorrelation for C9, the p-value was not adjusted with the Cochrane-Orcutt procedure.

3 Characterization of daily wind regimes

We split California into central and southern domains (Fig. 1) and identify 10 clusters for each domain. Each cluster describes a unique wind regime (a regional pattern of wind speeds and directions over the course of a day). Clusters are not linked between domains, e.g. C1 is not related to S1. The uniqueness of each cluster can be seen in the sample of four central California clusters shown in Fig. 3. One can see a striking difference, for example, in both the wind resources available and the general regional wind profile when comparing the two summer clusters (C1 and C7) showing typical marine air penetration (Wang and Ullrich 2018) conditions to the non-summer clusters showing flow from the north and east (C4) and showing typical conditions of a stagnant day (C9).

Although the clusters were developed based only on hub-height wind speed and direction, additional meteorological properties emerge which further distinguish and characterize each cluster. In Fig. 3, for example, C1 and C7 represent different flow conditions typical during the summer but are differentiated by an air temperature anomaly, as C7 corresponds to days with relatively higher temperatures than C1. Across the central and southern California domains we find distinct clusters associated with rainy storms, with stagnant days, and with cool or warm dry days. Of particular interest in southern California we found two clusters (S5 and S6) showing the distinct offshore flow associated with Santa Ana conditions. The Venn diagrams in Fig. 4 summarize these differences across the 10 clusters in each domain. Further details are provided in Supplemental Fig. 1 and 2 and Supplemental Tables 1 and 2.

Each cluster is associated with distinct synoptic scale patterns in geopotential height, pressure, air temperature, and wind flow. For example, in Fig. 5, we can see the anomaly from each monthly mean field in geopotential height, surface pressure and surface air temperature for the same group of clusters shown in Fig. 3. The synoptic scale patterns represent the average anomaly across all days associated with each cluster and are calculated separately by season. Each of the four clusters in Fig. 5 shows quite distinct synoptic-scale patterns. We note that the two clusters most commonly seen during the summer, C1 and C7, have relatively similar regional wind profiles but show almost opposite synoptic trends: the anomalies of geopotential height, surface pressure, and surface air temperature show the same spatial distribution but with opposite signs. C1 is associated with a negative anomaly in geopotential height centered off the Oregon coast, which enhances the flow of marine air into central California, cooling inland air temperatures. By contrast, the positive geopotential height anomaly field in C7 slightly suppresses on-shore flow condition, leading to an overall weaker marine air penetration as shown in Fig. 3. This example demonstrates how the clustering technique can illuminate meaningful differences between wind regimes even if those regimes share some similarities, such as the inflow patterns in C1 and C7.

The synoptic scale anomalies shown in Fig. 5 also help explain the conditions seen in the other two clusters shown (C4 and C9). C4 is cool and dry, occurring three to five days a month during the fall, winter, and spring. In Fig. 3, one can see that C4 is not a marine air penetration day, as

winds flow primarily from the north. Over the Sierra Nevada Mountains, winds flow from the east. Although high winds are seen in multiple locations within C4, the Fig. 3 diurnal profile inlay shows that winds at Shiloh and Altamont are distinctly muted in comparison to C1 and C7, with a relatively flat diurnal cycle with speeds peaking at 8 m s^{-1} . The synoptic scale anomalies driving these conditions (Fig. 5) show a high to low pressure gradient from north to south and a geopotential high in the north and low in the south. For C9, a low wind day across central California that occurs with a similar frequency and seasonal pattern to C4, the synoptic anomalies are equally distinct: Inland high pressure accompanied by a geopotential high centered slightly northeast of California.

We have now demonstrated that we can link wind speed profiles at specific wind project locations (the diurnal profile inlays in Fig. 3), to regional wind patterns (Fig. 3), as well as to synoptic scale conditions (Fig. 5). This linkage provides a useful framework with which to investigate variability in wind power resource – the focus of the next sections.

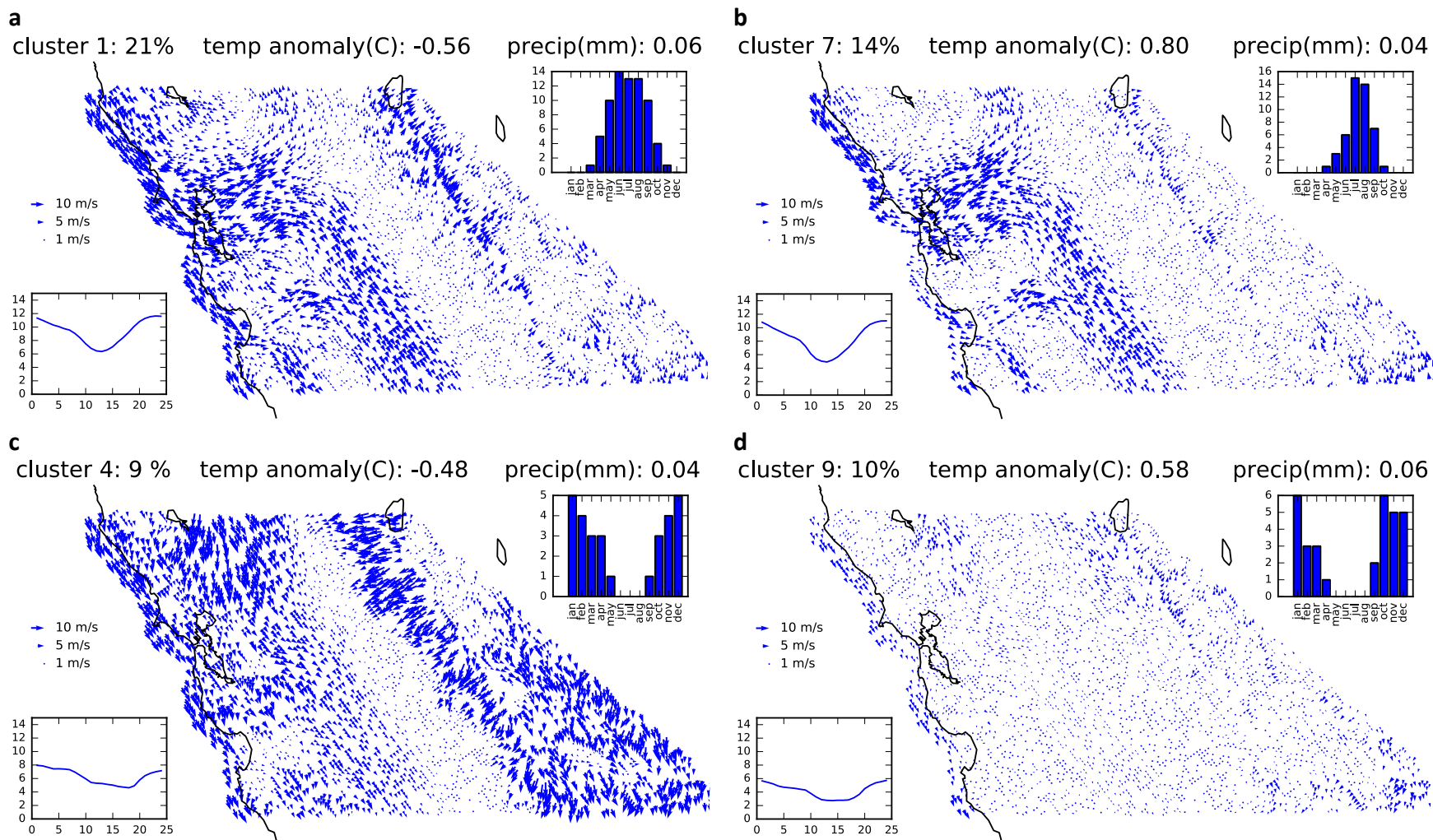


Fig. 3 Average wind vectors for a sample of the central California clusters. The upper right corner inlay the average number of days per month the cluster is found. The lower left corner inlay shows the average diurnal pattern (in Pacific Standard Time) of wind speed ($m s^{-1}$) at the grid cells centered on the Altamont Pass and Shiloh wind farms. The information across the top of each panel includes the cluster number, the percentage of the year each cluster is found, the average air temperature anomaly at the Altamont Pass and Shiloh wind farms (with the anomaly taken separately for each month and then averaged over the full-time span), and the average daily precipitation

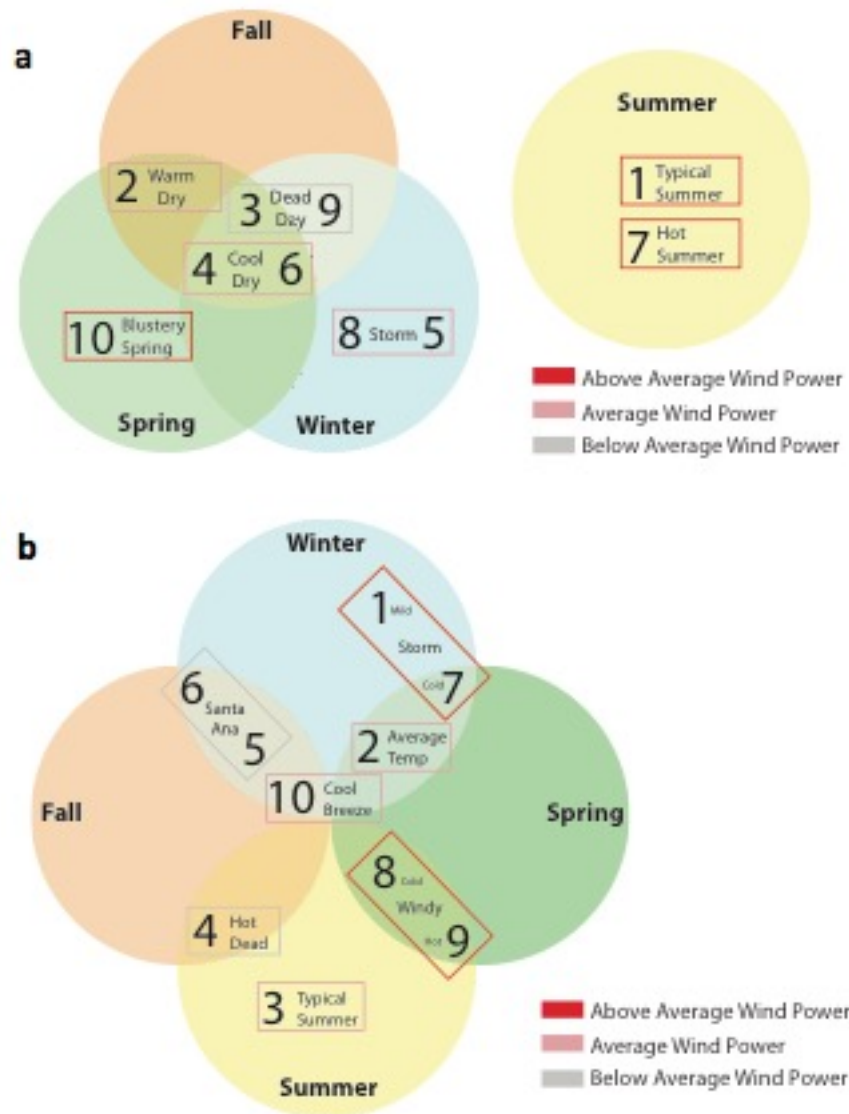


Fig. 4 Qualitative description of central (a) and southern (b) California wind regimes. Note that cluster numbers have no relationship between regions, e.g. C1 has no relationship to S1. The color of each box indicates relative energy potential of each regime based on the average energy potential of Shiloh and Altamont Pass for central California and Alta, San Gorgonio, and Ocotillo for southern California. Seasonal designations were chosen to indicate the time of year each cluster occurred most frequently, although most clusters were observed to occur (although less frequently) outside their designated seasons

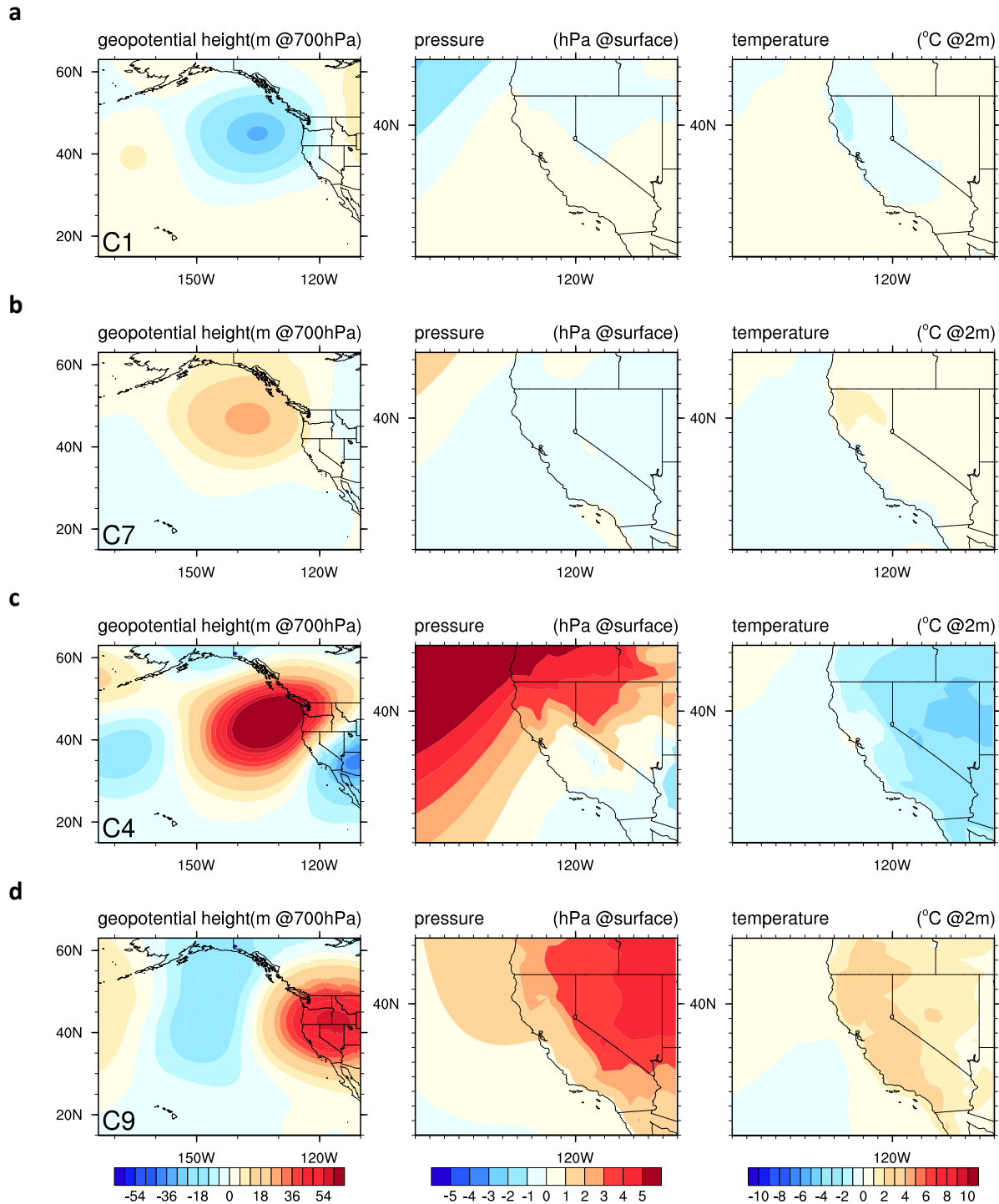


Fig. 5 Seasonal average synoptic-scale anomalies for 700-hPa geopotential height, surface pressure and 2-meter air temperature by cluster. (a), Cluster 1, averaged over June, July, and August. (b), Cluster 7 averaged over June, July, and August. (c), Cluster 4, averaged over September, October, and November. (d), Cluster 9, averaged over September, October, and November

1
2

4 Wind resource variability

A key concept describing wind resources is capacity factor (hereafter, CF). For a particular time period, CF is the ratio (expressed here in percentage terms) of energy generated by a turbine to the energy that same turbine could have generated had it been running at its rated capacity continuously (i.e., the MWh generated given actual wind speeds divided by the MWh that could have been generated with a constant ideal wind speed). In this case, we calculate a lossless CF based on using a power curve to estimate hourly generation as a function of wind speed (Sect. 2.4). We primarily compare capacity factors between time periods but within the same project (e.g., the average capacity factor of different cluster types or different years). Comparing within-project CF over an identical length of time is similar to comparing total energy yield. For example, if the capacity factor at Alta was 10% larger in one year compared to average, that would be equivalent to saying the energy yield at Alta was 10% larger in that year than average. Although comparing capacity factors across locations gives a rough guide to differences in potential energy yield, they are not equivalent because of differences in turbine and plant level characteristics. Wisser et al. (2017) contains a full discussion on how CF vary across plants and time in the U.S. A second metric, not to be confused with CF, but also in percentage terms, is the percent of total potential annual generation during a season or within a single cluster. We use this metric to compare the relative energy yield of one cluster to another, also within a single site, rather than between sites.

Across the five focus sites we see large variation in resource potential. At each site, we also see important variation by year. Average CF range from 57% at Alta to 31% at San Geronio, with the other sites falling within that range. CF varied by season and were higher in summer overall. This seasonality gives rise to 33% to 37% of annual generation occurring during July – August, across all the sites. An exception is at Alta, where only 28% of the total annual generation occurred during summer.

Variation in annual wind resource at each site is noteworthy. The ratio of the top year CF to the bottom year CF ranged from 1.19 at Alta to 1.47 at Ocotillo. Thus, in the most extreme case, the best year at Ocotillo would have produced almost 50% more energy than the worst year. More generally, the coefficient of variation was 3.9% at Shiloh, 4.9% at Altamont Pass, 4.2% at Alta, 7.8% at San Geronio, and 7.4% at Ocotillo.

Resources were correlated between sites. For example, the coefficient of determination comparing the annual CF of the three southern California sites ranged from 0.48 to 0.66. The central California sites, Shiloh and Altamont had lower correlation, with the corresponding coefficient of determination equaling 0.28. The southern sites showed little correlation with the central sites. Finally, we find no evidence of temporal trends in annual or seasonal CF at any of the sites from 1980 – 2015. Additional details related to site specific resource variability are included in Supplemental Tables 3 – 12.

We investigate resource variability and the mechanisms driving such variability using the clustering framework. First, we find the average CF of each cluster, and calculate the percent of

1 total generation potential from each cluster (Fig. 6). Most noticeable, the central California sites
2 (Shiloh and Altamont Pass) depend on only two clusters (C1 + C7, Fig. 3a and 3b) for about half
3 of their potential energy resource. These clusters represent two typical types of summertime
4 marine air penetration wind patterns. The rest of the energy potential at the central California
5 is split between storms (C5 + C8), warm fall and spring days (C2), and dead days (C3 + C9), each
6 accounting for ~10%, with cool and dry winter and spring like days (C4 + C6) accounting for
7 ~15%. We note that while generation potential at the two central California sites is similarly
8 divided between the weather regimes, correlation between the annual CF at the sites is not
9 particularly strong ($r^2 = 0.28$), thus the factors that drive inter-annual variability differ across
10 these sites.

11
12 At the southern California sites, specifically San Geronio and Ocotillo, windy spring-like
13 weather (S8 + S9) accounts for ~35% of total generation. Storms (S1 + S7), account for ~25% of
14 total generation and typical summer-like weather (S3) accounts for ~20% of annual generation.
15 Santa Ana type weather (S5 + S6) and dead days (S4) combined only account for ~10% of total
16 generation, but 35% of total days. At Alta, also in the southern California domain, the
17 distribution of generation across the clusters is similar to San Geronio and Ocotillo, although
18 one sees some differences for certain clusters (e.g., S2, S5, S8).

19
20 Most of the clusters we found span more than a single season, and in southern and central
21 California, each season was made up of multiple clusters. Thus, analyzing resource variability by
22 cluster allows one to investigate changes to weather patterns that might be obscured when
23 looking at resource variability on a seasonal basis.

24

25 **5 Top wind years vs. bottom wind years**

26

27 We compare cluster frequency and cluster CF found during the highest wind years to the lowest
28 wind years. We do this at each site and compare the top five to the bottom five wind resource
29 years. Through this comparison, we can identify the clusters that are most responsible for
30 differences in wind resource, and we can isolate whether the differences are caused by changes
31 to the frequency of the cluster or the within-cluster wind intensity (indicated by the cluster CF).
32 The source of resource variability differs strongly at each site.

33

34 At Altamont Pass, 38% more energy is produced on C1 days during top years versus bottom
35 years. Some of this increased energy production during C1 was due to an increase to within-
36 cluster wind speeds (at Altamont Pass: $CF_{C1-top}/CF_{C1-bottom} = 1.08$) but also, there were 19
37 additional C1 days, on average, per top-year. Correspondingly, there were 17 fewer C7-days per
38 top year. This switch is notable as C1 and C7 represent typical summer conditions, but are
39 associated with different regional and synoptic scale characteristics (Fig. 5). In particular, C7
40 represents hotter conditions compared to the cooler C1. There are other differences as well –
41 33% more energy was generated during stormy weather (C5 + C8) much of which is due to an
42 additional 12 days of storms during top years. To a lesser degree other clusters changed in
43 frequency as well (e.g., C9, 'dead days' occurred 6 fewer times during top years than bottom
44 years, a 16% reduction in frequency). Additionally, the average wind intensity within 8 of the 10

1 clusters was stronger during top years. Differences between top and bottom years are
2 summarized in Tables 1 and 2 with additional details provided in Supplemental Tables 3 – 12.

3
4 We can isolate the impact of top-bottom variation in within-cluster wind intensity, or cluster
5 frequency, by calculating hypothetical site-level annual capacity factors. The actual average top-
6 year CF (CF-top) is equal to the sum across clusters of $CF_i\text{-top} * AF_i\text{-top}$, where AF is the annual
7 fraction, $days_i/days\text{-per-year}$, of each cluster, with the subscript i referring to cluster number. If
8 instead we sum $CF_i\text{-bottom} * AF_i\text{-top}$ we isolate the impact of changing within-cluster wind
9 intensity (hereafter CF-wind). Likewise, summing $CF_i\text{-top} * AF_i\text{-bottom}$ isolates the impact of
10 changing cluster frequency (hereafter CF-freq). These calculations are simplistic as they ignore
11 interaction between cluster frequency and CF change, but they do give a general idea of the
12 relative importance of frequency versus intensity. At Altamont Pass we find that CF-wind and
13 CF-freq fall roughly in the middle between CF-top and CF-bottom (Table 2), indicating that both
14 frequency changes and within-cluster wind intensity changes play important roles in driving the
15 difference between top and bottom years. To summarize, at Altamont Pass, the primary
16 difference between top years and bottom years is an increased frequency of cooler typical
17 summer conditions at the expense of hotter summer conditions, also, top years had a greater
18 frequency of stormy days and a reduced frequency of dead days. Of roughly equal importance,
19 there is an increase to within-cluster wind speed across most of the clusters.

20
21 Shiloh, on the other hand, is almost entirely sensitive to changes to within-cluster wind speed:
22 the CF-freq is only 1% smaller than CF-top, whereas CF-wind and CF-bottom are 10% and 11%
23 smaller than CF-top, respectively (Table 2). The largest single factor in the difference between
24 top and bottom wind years derives from an increase to wind speeds within C1 ($CF_{C1}\text{-top}/CF_{C1}\text{-}$
25 $bottom = 1.23$). Thus, the primary factor driving top years at Shiloh is the intensity of the typical
26 summertime marine air penetration conditions (the regional and synoptic-scale structure that is
27 represented by C1). Of secondary importance is an increase to wind speeds in C4, C6, and C10,
28 clusters that represent typical springtime conditions, but not stormy conditions. Unlike
29 Altamont Pass, at Shiloh the ratio of CF-top to CF-bottom is insensitive to the storms (C5 and
30 C8) and to dead days (C3 and C9).

31
32 We see distinct differences between top and bottom years at the other three sites as well,
33 which, for the sake of brevity, we will describe more qualitatively. Alta is more sensitive to the
34 frequency of clusters than the within-cluster wind speeds. Specifically, top years at Alta have 26
35 more storm days (S1 and S7) and 10 additional hot windy spring days (S9). These come at the
36 expense of dead days (S4) and Santa Ana wind days (S5 and S6) which combined account for 43
37 fewer days on top years. The largest change to within cluster wind intensity is to storm cluster
38 S1: $CF_{S1}\text{-top}/CF_{S1}\text{-bottom} = 1.12$. Unlike Altamont Pass and Shiloh, Alta sees little difference in
39 either frequency or intensity of the typical summer conditions (S3) between top and bottom
40 years.

41
42 San Gorgonio and Ocotillo have similar differences between top and bottom years. They are
43 roughly equally sensitive to cluster frequency and within-cluster wind intensity changes. During
44 top years, San Gorgonio and Ocotillo each have ~20 additional storm (S1 and S7) and ~10

1 additional cold windy spring days (S8). These come at the expense of dead days (S4), Santa Ana
 2 days (S5 and S6) and hot windy spring days (S9). Additionally, the typical summer cluster (S3) is
 3 more frequent and has more intense wind speeds during top years at these sites.
 4

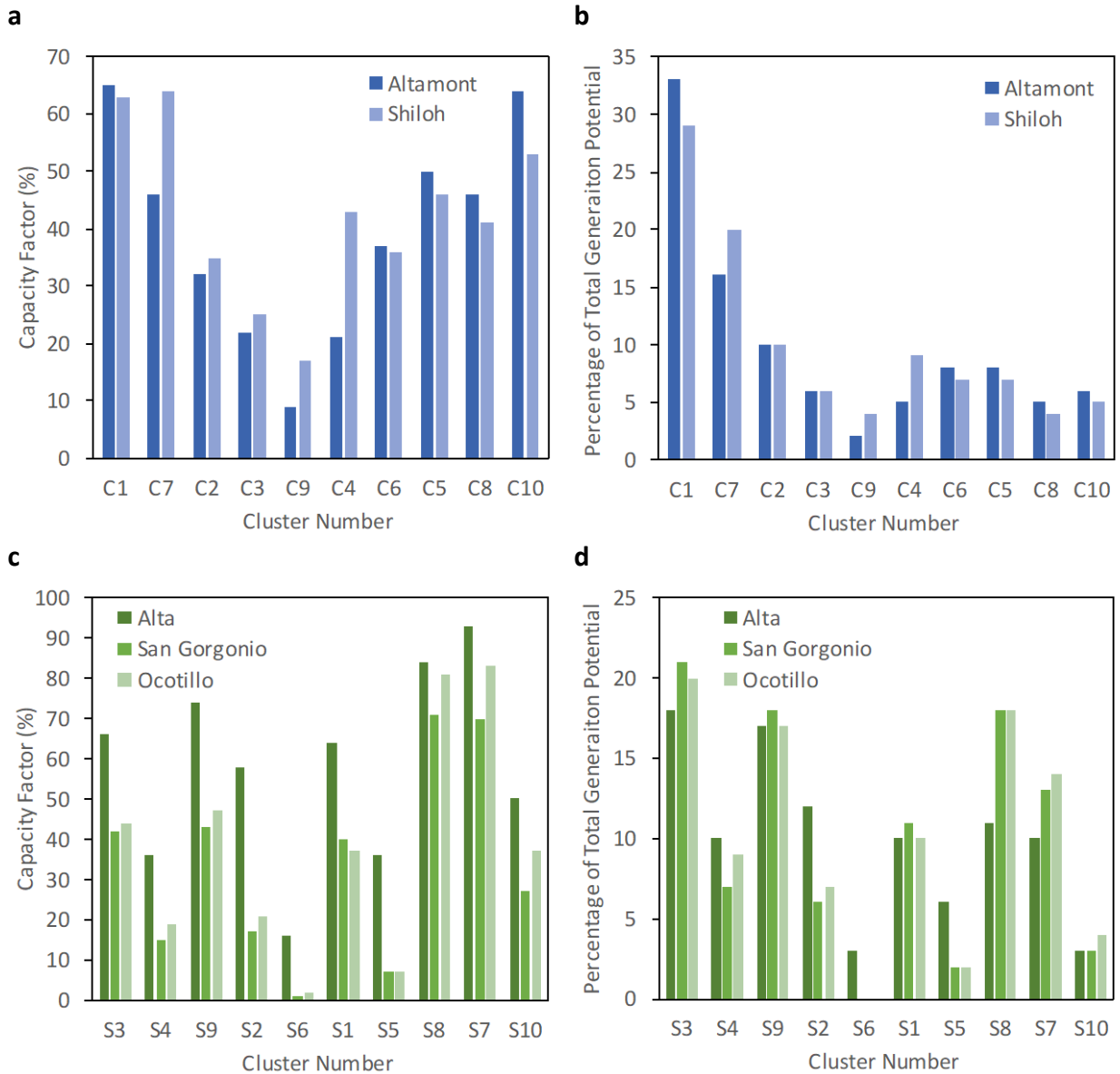


Fig. 6 Average capacity factor and percentage of total wind resource potential. (a) and (c), capacity factor by cluster. (b) and (d), percentage of total generation potential by cluster. (a) and (b), central California sites. (c) and (d), southern California sites. Note: clusters are shown in descending order, left to right, of the frequency of their occurrence

5

1 **Table 1** Average differences, in total days and in capacity factor, between the top five and bottom five wind years at each site. Differences are taken as the
 2 average top year value minus corresponding bottom year value. The ‘% of top-years energy’ is provided for context and is not a differenced quantity but simply
 3 the average percentage of total annual potential generation at each site corresponding to each cluster

	Central California						Southern California								
	Shiloh			Altamont Pass			Alta			San Gorgonio			Ocotillo		
	Δ Days	Δ CF (%)	% of top-years energy	Δ Days	Δ CF (%)	% of top-years energy	Δ Days	Δ CF (%)	% of top-years energy	Δ Days	Δ CF (%)	% of top-years energy	Δ Days	Δ CF (%)	% of top-years energy
C1 or S1	11.0	3.7	30.0	19.2	5.0	37.9	15.0	11.7	13.1	13.2	13.3	15.3	9.4	13.5	12.5
C2 or S2	-8.0	2.3	9.2	-11.4	6.0	9.0	8.4	-0.3	13.4	0.6	-0.6	5.2	-6.4	-2.3	5.6
C3 or S3	-7.2	4.7	6.2	-0.4	0.1	5.9	-0.6	2.3	17.8	6.8	7.5	18.7	5.2	7.2	19.2
C4 or S4	6.2	6.4	9.5	-8.8	3.3	4.1	-20.8	-0.6	7.6	-16.4	2.6	6.4	-13.6	3.0	7.9
C5 or S5	-3.8	9.6	5.9	6.2	4.4	9.0	-10.8	-1.1	4.2	-6.2	-0.5	1.4	-8.8	-0.6	1.2
C6 or S6	4.0	5.7	7.6	8.0	-2.1	7.2	-11.2	-2.8	1.4	-3.6	-0.3	0.2	0.8	-0.7	0.3
C7 or S7	-4.0	3.9	18.5	-17.2	2.5	10.7	11.4	1.7	11.5	10.4	6.4	17.5	10.8	1.2	16.7
C8 or S8	-2.4	5.8	4.1	6.2	3.7	6.8	4.0	1.4	11.2	7.8	2.6	17.3	10.2	3.7	17.5
C9 or S9	2.8	1.3	4.1	-6.2	6.9	2.6	10.2	6.6	17.2	-9.8	9.9	15.3	-7.8	10.3	15.8
C10 or S10	2.0	11.5	4.9	4.2	4.3	6.9	-5.4	2.8	2.5	-3.2	3.0	2.7	-0.4	5.8	3.4

4
 5 **Table 2** Average annual capacity factors and the influence of changes to wind regime frequency and intensity on annual capacity factor during top five and
 6 bottom five wind years at each site

	CF-top (%)	CF-wind (%)	CF-freq (%)	CF-bottom (%)
Shiloh	47.0	42.4	46.4	41.9
Altamont Pass	43.2	39.6	40.4	36.7
Alta	60.6	58.1	54.8	53.0
San Gorgonio	36.0	31.0	32.2	27.7
Ocotillo	39.3	34.7	35.1	30.9

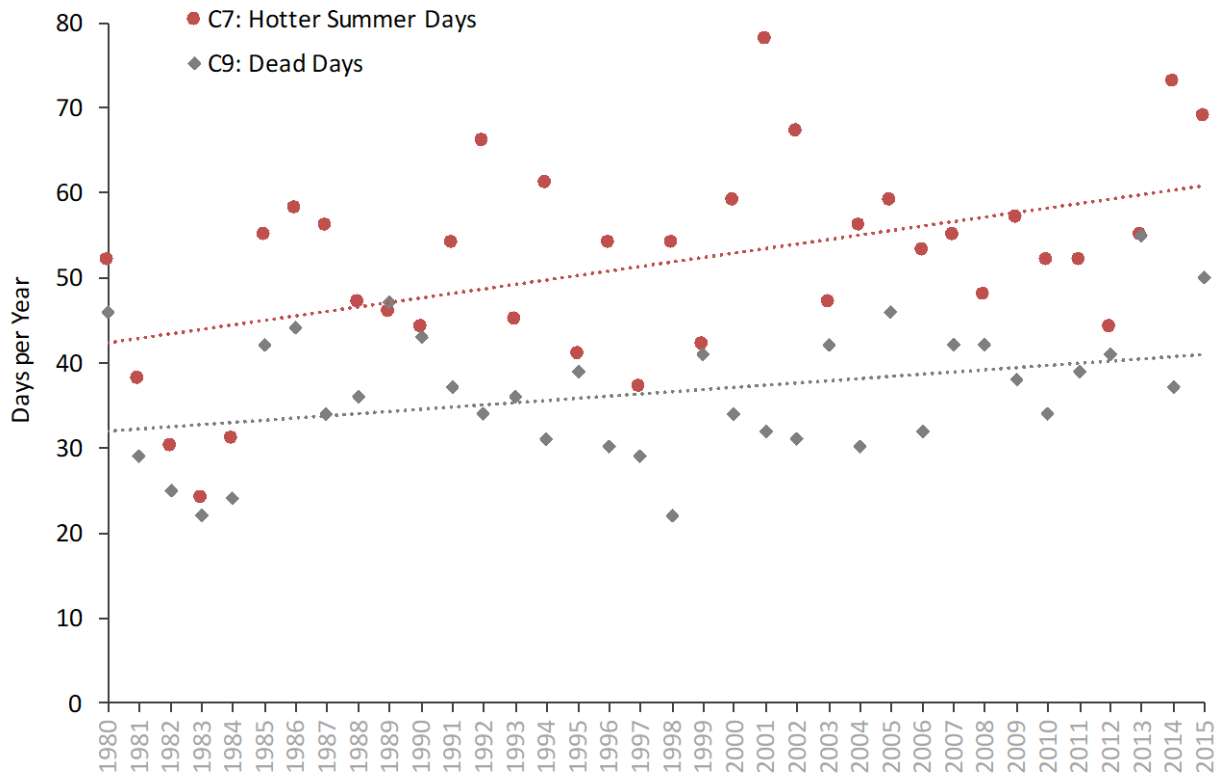
7
 8

1 **6 Wind resource variability links to climate change**

2

3 While we found no evidence of temporal trends in energy resources at the seasonal or annual
4 level, we do see evidence for trends in cluster frequency. Specifically, we found that the
5 frequencies of C7, hot summer conditions, and C9, non-summer dead days, were increasing at a
6 rate of roughly one half and one fourth day per year (Fig. 7), respectively. The trend for C7 and
7 C9 was found to be significant at the 95% level (p-value of 0.012 and 0.039, respectively, see
8 sect. 2.5). The increased frequency of C7 and C9 came at the expense of all other clusters,
9 which were found to have a decline frequency over time, excepting C3, but these results were
10 not statistically significant. Despite the result of statistical significance for C7 and C9, this time-
11 series analysis is based only on 36 data points (1 per year) and thus potentially influenced by
12 decadal or multi-decadal climate modes, and so conclusions should be treated cautiously.
13 Notably, we did not find strong evidence of temporal trends in cluster frequency in southern
14 California.

15



16

17 **Fig. 7** C7 and C9 increase in frequency overtime. For each cluster, the dotted lines correspond
18 to a simple linear regression of days per year with year

19

20 The changes to C7 and C9 are generally consistent with a signal of global warming. Stagnant
21 conditions (i.e. C9) are forecast to increase across the western U.S. throughout the 21st century
22 (Horton et al. 2014; Jacob and Winner 2009). In central California, Wang et al. (2018) found that
23 climate change may favor the synoptic scale patterns that create marine air penetration events
24 (i.e. C7). One additional observation consistent with global warming: both C7 and C9 are

1 associated with warmer than average air temperatures having positive temperature anomalies
2 of 0.79 °C and 0.58 °C, respectively, yet the similar clusters representing marine air penetration
3 events (C1) and stagnation events (C3) during days with negative temperature anomalies show
4 no evidence of increased frequency overtime.

5
6 If this pattern is maintained into the future, it represents an important change to weather
7 patterns in central California. Increasing at half a day per year, C7 occurs ~18 days more per
8 year at the end of the period than the beginning, and this change is focused on a narrow
9 portion of the year, as C7 occurs mostly during summer months. The ~9 day increase in C9
10 during the time period is also important, and focused on non-summer months. In particular, the
11 increase in C9 dead days may have important implications for air quality (Dawson et al. 2014;
12 Leung and Gustafson 2005; Mickley et al. 2004; Sun et al. 2017). More generally, since the
13 clusters did not ingest temperature, the change in cluster frequency is suggestive that shifts in
14 wind patterns may be an additional impact due to climate change beyond temperature
15 increases.

16
17 What are the implications of these changes for wind energy? At Altamont Pass, we found that
18 low wind years had an additional ~17 days of the C7 cluster. Thus, the increasing C7 frequency
19 might imply that the frequency of low wind years also increased with time. However, low wind
20 years saw increased C7 days explicitly at the expense of decreased C1 days while the long-term
21 increase observed in C7 frequency came at the expense of all other clusters (as opposed to only
22 C1). Because C7 is ranked 5 out of 10 for generation potential at Altamont Pass, the broad shift
23 towards additional C7 had little impact on average annual wind resource potential.

24
25 C7 has the highest wind generation potential of any cluster at Shiloh, thus, we might expect
26 some positive change in resource potential at Shiloh. However, we do not see a significant
27 signal in average summer CF at Shiloh. The lack of increase in summer time resource potential is
28 consistent with the finding that differences between strong and weak years at Shiloh were most
29 sensitive to within cluster intensity rather than cluster distribution.

30
31 Finally, at both sites, we might expect the increase in C9 days to lead to a decreased non-
32 summer energy potential. However, we do not see a significant signal in the average non-
33 summer seasonal CF. As the additional C9 days are spread across three seasons, the change
34 within a single season is small compared to each season's variability.

35
36 Of course, if these trends continue, a change to seasonal power generation may be seen in the
37 future. Additional research will be needed to determine if the changes shown here are early
38 indicators of the changes to wind energy resources in California forecasted by Duffy et al.
39 (2014) and Wang et al. (2018). In particular, the results described above are not inconsistent
40 with the findings by Wang et al. (2018) of increased future wind resources across the state
41 during the summer (June through August) but decreased wind resources across the state in the
42 fall and winter (September through February).

1
2
3
4
5
6
7
8
9
10
11
12
13
14
15
16
17
18
19
20
21
22
23
24
25
26
27
28
29
30
31
32
33
34
35
36
37
38
39
40
41
42
43
44

7 Wind resource variability links to climate mode

Here, we look for links between wind energy resources and climate modes (climate modes are identifiable, large-scale climate patterns that impact regional weather). Similar to the previous section, we did not find evidence of correlation between seasonal average CF and climate modes, however we did find evidence that the frequency of a number of clusters in both central and southern California were linked to climate mode indices. The correlation is based on a simple, single variable, linear regression between season average cluster frequencies and seasonal average climate indices. Additional measures and techniques may bear insight into possible links between climate variability and wind resource variability. For example, this study does not consider correlations on sub-seasonal timescales, the possibility of lagged responses, interactions between multiple climate modes and cluster frequency, nor the inter-correlation of climate modes themselves. However, the results presented here demonstrate at a high level the connections between cluster frequency and climate mode, while more complex analysis should be considered when developing explicit forecasting approaches.

We report the percentage increase to seasonal frequency of clusters in response to a shift from -1.0 to +1.0 in the associated climate mode index. All values reported are statistically significant at the 95% level unless otherwise stated. For each season, we tested correlations between each cluster and the monthly indices of five climate modes, the El Niño Southern Oscillation (ENSO), the Pacific North American (PNA) pattern, the North Atlantic Oscillation (NAO), the Arctic Oscillation (AO), and the Pacific Decadal Oscillation (PDO), (NOAA 2017a; NOAA 2017b; NOAA 2017c; NOAA 2017d; NOAA 2017e) .

As expected, during winter, storm clusters C8 and S1 increased in frequency with ENSO, by 45% and 30%, respectively, however the S1 correlation was not statistically significant with a p-value of 0.052. C8 also increased by 74% during winter with PNA. Interestingly, storm clusters C5 and S7 were not correlated with ENSO, indicating that perhaps the clusters are picking out storms with different origins. The southern California storm cluster that was correlated with ENSO (S1) is more common than the southern California storm cluster not correlated with ENSO (S7). S7 is also distinctly colder than S1, having an air temperature anomaly of -3.5° versus 0.2 °C. The distinction between the central California storm clusters C5 and C8 is not immediately obvious.

The impact on wind energy resources from the correlations between ENSO and PNA with storm clusters is muted in central California because wind resources at Altamont Pass and Shiloh are not particularly sensitive to the frequency of storm days. That is, Altamont Pass was most sensitive to the relative frequency of the two types of summer-like clusters C1 vs. C7 and Shiloh was most sensitive to the within-cluster wind intensity, rather than to a shift in the distribution of cluster types. Wind resources at the three sites in southern California are potentially sensitive to the connection between S1 frequency and El Niño, as S1 provides a significant portion of total energy resource at each site and occurs more frequently during strong wind years than weak wind years (e.g., 15 and 13 additional S1 days occur at Alta and San Geronio, respectively, during strong wind years over weak wind years). Despite this potential impact

1 from additional S1 days, there was no significant correlation found between ENSO and winter
2 CF at any of the southern California sites.

3
4 In addition to increased storms during winter, Berg et al. (2013) found that Santa Ana events
5 decreased in frequency during El Niño winters. It is therefore interesting to note that while we
6 did see nominally fewer Santa Ana events during El Niño winters compared with La Niña
7 winters, 33 vs. 35, the result was not significant. However, the definition of Santa Ana events,
8 here defined as cluster S5 and S6, was not exactly equivalent to the definition in Berg et al.
9 (2013), in which Santa Ana winds were one of only three total cluster types.

10
11 Additional teleconnections were found in both central and southern California domains,
12 however, unlike the correlations between storms and ENSO and PNA, we have no a priori
13 reasons to expect these additional teleconnections. Therefore, due to issues of multiplicity, we
14 cannot assume these correlations are statistically significant despite individual test p-values
15 below 0.05. Still, a brief description of some of the most prominent correlations may be useful
16 as context for future research.

17
18 In central California, additional teleconnections include dead days (C3 and C9) and hot summer
19 days (C7). During the fall, C3 increased by 40% with PNA and C9 increased by 35% with NAO.
20 Another correlation found was that C7 increased by ~70% with both AO and NAO during the
21 Spring. The increase to C7 did not correspond to a decrease in a single other cluster, but instead
22 C7 substituted for a number of different clusters (i.e., there were no clusters that showed a
23 significant springtime decrease with either AO or NAO). In southern California, we found that
24 typical warm summer days, S3, increased by 50% with ENSO during the spring. Additionally, S7
25 correlated with NAO decreasing by 45% in the spring season. We found no evidence of
26 teleconnections between climate modes and the central or southern California clusters during
27 the summer season.

28 29 **8 Conclusions**

30
31 In this work, we demonstrate that analyzing wind resource variability with a clustering
32 framework can (1) provide a direct, intuitive, link between local wind resources and regional
33 and synoptic scale meteorological patterns, (2) provide insight in to the meteorological patterns
34 driving the differences between weak and strong wind years, and (3) help elucidate the impacts
35 of climate modes and climate change on local and regional wind resources.

36
37 To demonstrate conclusion 1, we showed how each cluster was associated with unique
38 synoptic scale conditions, and also with a particular local diurnal cycle of wind energy resource.
39 While these clusters were devised purely on the regional and diurnal pattern of wind speeds,
40 they were associated with distinct local meteorological patterns of air temperature and
41 precipitation. One point of interest was that even the few clusters that shared broadly similar
42 regional wind patterns and seasonality patterns had noticeably different average synoptic scale
43 conditions.

1 Related to conclusion 2, we compared the distributions of clusters across strong and weak wind
2 resource years. At Shiloh, we found that the distribution of cluster types changed little between
3 strong and weak wind resource years, but that certain cluster types exhibited weaker winds
4 during weak years. For example, at Shiloh, winds within the typical summertime cluster C1
5 were 23% greater during strong years than weak years. At Altamont Pass we found that in
6 comparison to weak years, strong years were marked by an increase in cooler typical summer
7 days (C1) at the expense of hotter summer days (C7). At Alta, the difference between strong
8 and weak years was mostly dependent on the cluster distribution, for example, top years at
9 Alta had 26 more storm type days, and many fewer Santa Ana wind days. The difference
10 between strong years and weak years at Altamont Pass, San Geronimo and Ocotillo, was due to
11 a combination of weaker winds within certain cluster types and changes to the distribution of
12 cluster type. For example, during strong years, San Geronimo and Ocotillo had additional storm
13 days and also more intense winds during typical summer days. Identifying the above drivers of
14 low and top wind years is a unique aspect of this work, and provides a ready starting point for
15 future efforts to investigate the causes of, and develop the ability to predict, such inter-annual
16 variability.

17
18 Related to conclusion 3, we found significant correlation between the frequency of particular
19 cluster types and the intensity of certain climate modes. We also found a significant increase in
20 the frequency of particular clusters over time. These trends existed in the cluster frequency
21 distribution, but not in the total average wind resources, e.g., there was no temporal trend in
22 total potential annual energy generation over time at any of the sites. Of particular note, we
23 saw a long-term increase to low-wind 'dead' days and hot summer-type days in central
24 California. It is possible the increase in those types of days is related to climate change,
25 although further research would be necessary to confirm that assertion. Should those types of
26 days continue to increase overtime it would have a number of impacts on wind energy
27 resources. These potential impacts would likely vary by site and season. Finally, we found, as
28 expected, that storm cluster frequency correlated with El Niño intensity during winter seasons.
29 However, in each domain, only one of the multiple clusters associated with storms was found
30 to increase with El Niño, pointing to possibility that the storm clusters were associated with
31 storms from differing origins. A number of other, possibly significant, correlations between
32 climate modes and cluster frequency were found during the fall and spring, for example, low
33 wind 'dead' days increased with the Pacific North American pattern and the North Atlantic
34 Oscillation in the fall in Central California. These types of teleconnections deserve additional
35 study and may become a useful input for models attempting seasonal predictions of wind
36 energy.

37
38 It is a limitation of this research that the results are dependent on a single meteorological
39 simulation. However, the Virtual Met product evaluation described in the Methods provides
40 some confidence in our representation of the wind fields. Additionally, the unique synoptic
41 conditions associated with each cluster type also provides evidence that the approach applied
42 here provides useful classification of weather types that may be robust across approaches.
43 Future research in this area may compare results across meteorological products, and also
44 across clustering techniques to determine the robustness of these results.

1 We believe this clustering framework could be used in a number of applications within the wind
2 industry, as well as more generally in the atmospheric science and air quality communities.
3 Most immediately, the framework could be used to help explain the causes for particularly
4 anomalous wind resource periods. Future research could determine if the clustering framework
5 could be included in the early stages of site-level wind resource assessment, possibly as a
6 refinement of the measure-correlate-predict process. Future research could also determine if
7 the synoptic scale link to local wind resource patterns may be useful for short term, low
8 computational cost, wind resource forecasting. Most generally, the framework allows for an
9 accounting of wind resource variability that is not bound artificially to seasonal or monthly
10 time-periods, directly links local wind patterns to regional and synoptic scale patterns, is
11 intuitive and accessible, yet quantitative and repeatable in any location.
12
13

1
2
3
4
5
6
7
8
9

Acknowledgements This work was funded by the California Energy Commission under the Electric Program Investment Charge grant, “EPC-15-068: Understanding and Mitigating Barriers to Wind Energy Expansion in California.” We would like to thank Chris Hayes and Daran Rife of DNV GL for helpful discussions. And from Lawrence Berkeley National Laboratory, we thank Aditya Murthi for early input into this research and Samir Touzani for helpful discussion about the methodological approach. This research used resources of the National Energy Research Scientific Computing Center, a DOE Office of Science User Facility supported by the Office of Science of the U.S. Department of Energy under Contract No. DE-AC02-05CH11231.

1 **References**

- 2
- 3 Albadi M, El-Saadany E (2010) Overview of wind power intermittency impacts on power
4 systems. *Electric Power Systems Research* 80:627-632
- 5 Archer CL, Jacobson MZ (2013) Geographical and seasonal variability of the global “practical”
6 wind resources. *Applied Geography* 45:119-130
7 doi:<https://doi.org/10.1016/j.apgeog.2013.07.006>
- 8 Archer CL, Simão HP, Kempton W, Powell WB, Dvorak MJ (2017) The challenge of integrating
9 offshore wind power in the U.S. electric grid. Part I: Wind forecast error. *Renewable*
10 *Energy* 103:346-360 doi:<https://doi.org/10.1016/j.renene.2016.11.047>
- 11 Bailey B, Kunkel J (2015) *The Financial Implications of Resource Assessment Uncertainty*. North
12 American Windpower. vol 12.
- 13 Barthelmie R, Pryor S (2014) Potential contribution of wind energy to climate change
14 mitigation. *Nat Clim Change* 4:684-688
- 15 Beaver S, Palazoglu A (2009) Influence of synoptic and mesoscale meteorology on ozone
16 pollution potential for San Joaquin Valley of California. *Atmos Environ* 43:1779-1788
- 17 Berg N, Hall A, Capps SB, Hughes M (2013) El Niño-Southern Oscillation impacts on winter winds
18 over Southern California. *Climate dynamics* 40:109-121
- 19 Bolinger M (2017) *Using Probability of Exceedance to Compare the Resource Risk of Renewable*
20 *and Gas-Fired Generation*. Lawrence Berkeley National Laboratory.
- 21 Carta JA, Velázquez S, Cabrera P (2013) A review of measure-correlate-predict (MCP) methods
22 used to estimate long-term wind characteristics at a target site. *Renew Sustainable*
23 *Energy Rev* 27:362-400
- 24 Chadee XT, Clarke RM (2015) Daily near-surface large-scale atmospheric circulation patterns
25 over the wider Caribbean. *Climate Dynamics* 44:2927-2946
- 26 Clifton A, Lundquist JK (2012) Data clustering reveals climate impacts on local wind phenomena.
27 *Journal of Applied Meteorology and Climatology* 51:1547-1557
- 28 Cochran J, Mai T, Bazilian M (2014) Meta-analysis of high penetration renewable energy
29 scenarios. *Renew Sustainable Energy Rev* 29:246-253
- 30 Cochrane D, Orcutt GH (1949) Application of Least Squares Regression to Relationships
31 Containing Auto-Correlated Error Terms. *Journal of the American Statistical Association*
32 44:32-61 doi:10.1080/01621459.1949.10483290
- 33 Conil S, Hall A (2006) Local regimes of atmospheric variability: A case study of southern
34 California. *Journal of Climate* 19:4308-4325
- 35 Cullen J (2013) Measuring the environmental benefits of wind-generated electricity. *AEJ: Econ*
36 *Pol* 5:107-133
- 37 Darby LS (2005) Cluster analysis of surface winds in Houston, Texas, and the impact of wind
38 patterns on ozone. *Journal of Applied Meteorology* 44:1788-1806
- 39 Dawson JP, Bloomer BJ, Winner DA, Weaver CP (2014) Understanding the meteorological
40 drivers of US particulate matter concentrations in a changing climate. *Bulletin of the*
41 *American Meteorological Society* 95:521-532
- 42 Delle Monache L, Eckel FA, Rife DL, Nagarajan B, Searight K (2013) Probabilistic weather
43 prediction with an analog ensemble. *Monthly Weather Review* 141:3498-3516

1 Delle Monache L, Nipen T, Liu Y, Roux G, Stull R (2011) Kalman filter and analog schemes to
2 postprocess numerical weather predictions. *Monthly Weather Review* 139:3554-3570

3 Draxl C, Clifton A, Hodge B-M, McCaa J (2015) The wind integration national dataset (WIND)
4 Toolkit. *Appl Energy* 151:355-366

5 Duffy PB, Bartlett J, Dracup J, Freedman J, Madani K, Waight K (2014) Climate Change Impacts
6 on Generation of Wind, Solar, and Hydropower in California. California Energy
7 Commission.

8 Gelaro R et al. (2017) The modern-era retrospective analysis for research and applications,
9 version 2 (MERRA-2). *Journal of Climate* 30:5419-5454

10 GES (2017) Goddard Earth Sciences Data and Information Services Center. MERRA-2 inst3 3d
11 asm Np: 3d,3-Hourly,Instantaneous,Pressure- Level,Assimilation,Assimilated
12 Meteorological Fields V5.12.4. DOI: 10.5067/QBZ6MG944HW0.

13 Gibson PB, Cullen NJ (2015) Synoptic and sub-synoptic circulation effects on wind resource
14 variability—A case study from a coastal terrain setting in New Zealand. *Renewable
15 Energy* 78:253-263

16 Goddard SD, Genton MG, Hering AS, Sain SR (2015) Evaluating the impacts of climate change on
17 diurnal wind power cycles using multiple regional climate models. *Environmetrics*
18 26:192-201

19 GWEC (2017) Global Wind Report: Annual Market Update 2016. Global Wind Energy Council.

20 Haupt SE, Copeland J, Cheng WY, Zhang Y, Ammann C, Sullivan P (2016) A Method to Assess the
21 Wind and Solar Resource and to Quantify Interannual Variability over the United States
22 under Current and Projected Future Climate. *Journal of Applied Meteorology and
23 Climatology* 55:345-363

24 Horton DE, Skinner CB, Singh D, Diffenbaugh NS (2014) Occurrence and persistence of future
25 atmospheric stagnation events. *Nat Clim Change* 4:698-703

26 Jacob DJ, Winner DA (2009) Effect of climate change on air quality. *Atmos Environ* 43:51-63

27 Jiménez PA, González-Rouco JF, Montávez JP, García-Bustamante E, Navarro J (2009)
28 Climatology of wind patterns in the northeast of the Iberian Peninsula. *International
29 Journal of Climatology* 29:501-525

30 Jin L, Harley RA, Brown NJ (2011) Ozone pollution regimes modeled for a summer season in
31 California's San Joaquin Valley: A cluster analysis. *Atmos Environ* 45:4707-4718

32 Kaffine DT, McBee BJ, Lieskovsky J (2013) Emissions savings from wind power generation in
33 Texas. *Energy J* 34:155

34 Karnauskas KB, Lundquist JK, Zhang L (2017) Southward shift of the global wind energy resource
35 under high carbon dioxide emissions. *Nature Geoscience* doi:10.1038/s41561-017-0029-
36 9

37 Leung LR, Gustafson WI (2005) Potential regional climate change and implications to US air
38 quality. *Geophysical Research Letters* 32

39 Li X, Zhong S, Bian X, Heilman W (2010) Climate and climate variability of the wind power
40 resources in the Great Lakes region of the United States. *Journal of Geophysical
41 Research: Atmospheres* 115

42 Luderer G et al. (2014) The role of renewable energy in climate stabilization: results from the
43 EMF27 scenarios. *Climatic Change* 123:427-441 doi:10.1007/s10584-013-0924-z

- 1 Ludwig FL, Horel J, Whiteman CD (2004) Using EOF analysis to identify important surface wind
2 patterns in mountain valleys. *Journal of Applied Meteorology* 43:969-983
- 3 McVicar TR, Van Niel TG, Li LT, Roderick ML, Rayner DP, Ricciardulli L, Donohue RJ (2008) Wind
4 speed climatology and trends for Australia, 1975–2006: Capturing the stilling
5 phenomenon and comparison with near-surface reanalysis output. *Geophysical
6 Research Letters* 35
- 7 Mickley LJ, Jacob DJ, Field B, Rind D (2004) Effects of future climate change on regional air
8 pollution episodes in the United States. *Geophysical Research Letters* 31
- 9 Millstein D, Wiser R, Bolinger M, Barbose G (2017) The climate and air-quality benefits of wind
10 and solar power in the United States. *Nature Energy* 2:17134
- 11 NOAA (2017a) Arctic Oscillation (AO). National Oceanic and Atmospheric Administration.
12 <https://www.ncdc.noaa.gov/teleconnections/ao/>.
- 13 NOAA (2017b) Historical El Nino / La Nina episodes (1950-present) National Oceanic and
14 Atmospheric Administration.
15 http://origin.cpc.ncep.noaa.gov/products/analysis_monitoring/ensostuff/ONI_v5.php.
- 16 NOAA (2017c) North Atlantic Oscillation (NAO). National Oceanic and Atmospheric
17 Administration. <https://www.ncdc.noaa.gov/teleconnections/nao/>.
- 18 NOAA (2017d) Pacific Decadal Oscillation (PDO). National Oceanic and Atmospheric
19 Administration. <https://www.ncdc.noaa.gov/teleconnections/pdo/>.
- 20 NOAA (2017e) Pacific-North American (PNA). National Oceanic and Atmospheric
21 Administration. <https://www.ncdc.noaa.gov/teleconnections/pna/>.
- 22 Olauson J, Edström P, Rydén J (2017) Wind turbine performance decline in Sweden. *Wind
23 Energy* 20:2049-2053
- 24 Pedregosa F et al. (2011) Scikit-learn: Machine learning in Python. *Journal of Machine Learning
25 Research* 12:2825-2830
- 26 Pryor S, Barthelmie R (2011) Assessing climate change impacts on the near-term stability of the
27 wind energy resource over the United States. *Proc Natl Acad Sci USA* 108:8167-8171
- 28 Pryor S, Barthelmie R (2013) Assessing the vulnerability of wind energy to climate change and
29 extreme events. *Climatic change* 121:79-91
- 30 Pryor S et al. (2009) Wind speed trends over the contiguous United States. *Journal of
31 Geophysical Research: Atmospheres* 114
- 32 Pryor S, Barthelmie RJ, Schoof J (2006) Inter-annual variability of wind indices across Europe.
33 *Wind Energy* 9:27-38
- 34 Seefeldt MW, Cassano JJ, Parish TR (2007) Dominant regimes of the Ross Ice Shelf surface wind
35 field during austral autumn 2005. *Journal of Applied Meteorology and Climatology*
36 46:1933-1955
- 37 Sherman P, Chen X, McElroy MB (2017) Wind-generated Electricity in China: Decreasing
38 Potential, Inter-annual Variability and Association with Changing Climate. *Scientific
39 Reports* 7:16294 doi:10.1038/s41598-017-16073-2
- 40 Siler-Evans K, Azevedo IL, Morgan MG, Apt J (2013) Regional variations in the health,
41 environmental, and climate benefits of wind and solar generation. *Proc Natl Acad Sci
42 USA* 110:11768-11773
- 43 Staffell I, Green R (2014) How does wind farm performance decline with age? *Renewable
44 energy* 66:775-786

1 Sun W, Hess P, Liu C (2017) The impact of meteorological persistence on the distribution and
2 extremes of ozone. *Geophysical Research Letters* 44:1545-1553

3 Tindal A Financing Wind Farms and the Impacts of P90 and P50 Yields. In: EWEA Wind Resource
4 Assessment Workshop, 2011.

5 Vautard R, Cattiaux J, Yiou P, Thépaut J-N, Ciais P (2010) Northern Hemisphere atmospheric
6 stilling partly attributed to an increase in surface roughness. *Nature Geoscience* 3:756

7 Wang M, Ullrich P (2018) Marine air penetration in California's Central Valley: Meteorological
8 drivers and the impact of climate change. *Journal of Applied Meteorology and*
9 *Climatology* 57:137 - 154

10 Wang M, Ullrich P, Millstein D (2018) The future of wind energy in California: Future projections
11 with the Variable-Resolution CESM. *Renewable Energy* 127:242 - 257

12 Ward Jr JH (1963) Hierarchical grouping to optimize an objective function. *Journal of the*
13 *American statistical association* 58:236-244

14 Wisner R et al. (2017) 2016 Wind Technologies Market Report. U.S. Department of Energy,
15 Wisner R, Jenni K, Seel J, Baker E, Hand M, Lantz E, Smith A (2016) Expert elicitation survey on
16 future wind energy costs. *Nature Energy* 1:16135

17 Xie L, Carvalho PM, Ferreira LA, Liu J, Krogh BH, Popli N, Ilic MD (2011) Wind integration in
18 power systems: Operational challenges and possible solutions. *Proceedings of the IEEE*
19 99:214-232

20 Yu L, Zhong S, Bian X, Heilman WE (2015) Temporal and spatial variability of wind resources in
21 the United States as derived from the Climate Forecast System Reanalysis. *Journal of*
22 *Climate* 28:1166-1183

23 Yu L, Zhong S, Bian X, Heilman WE (2016) Climatology and trend of wind power resources in
24 China and its surrounding regions: a revisit using Climate Forecast System Reanalysis
25 data. *International Journal of Climatology* 36:2173-2188

26 Zaremba LL, Carroll JJ (1999) Summer wind flow regimes over the Sacramento Valley. *Journal of*
27 *Applied Meteorology* 38:1463-1473

28